Three Crystal Structures of Vacuum-Dehydrated Zeolite X, $M_{46}Si_{100}Al_{92}O_{384}$, M = Mg^{2+}, Ca^{2+}, and Ba^{2+}

Young Hoon Yeom, Se Bok Jang, and Yang Kim*

Department of Chemistry, Pusan National University, Pusan 609-735, Korea

Seong Hwan Song

Department of Chemical Engineering, Dongseo University, Pusan 616-010, Korea

Karl Seff*

Department of Chemistry, University of Hawaii, 2545 The Mall, Honolulu, Hawaii 96822

Received: May 10, 1996; In Final Form: March 11, 1997[⊗]

The crystal structures of vacuum-dehydrated, fully Mg^{2+}-, Ca^{2+}-, and Ba^{2+}-exchanged zeolite X ($Mg_{46}(H_2O)_4$−X, Ca_{46}−X, and Ba_{46}−X; X = $Si_{100}Al_{92}O_{384}$) have been determined by single-crystal X-ray diffraction techniques in the cubic space group $Fd\bar{3}$ at 21 °C (a = 24.671(5), 25.024(4), and 25.266(5) Å, respectively). Their structures were refined to the final error indices R_w = 0.046 with 439 reflections, 0.037 with 434 reflections, and 0.049 with 485 reflections, respectively, for which $I > 3\sigma(I)$. In $Mg_{46}(H_2O)_4$−X, Mg^{2+} ions are found at four crystallographic sites: 14 per unit cell are located at site I at the center of the hexagonal prism (Mg−O = 2.262(6) Å), only four are at site I′ in the sodalite cavity near the hexagonal prism (Mg−O = 2.221(5) Å), four, each coordinated to an H_2O molecule, are located at site II′ in the sodalite cavity (Mg−O = 2.223(12) Å), and the remaining 24 are at site II near single six-oxygen rings in the supercage (Mg−O = 2.184(5) Å). In Ca_{46}−X, Ca^{2+} ions are found at only two sites: 16 per unit cell fill site I (Ca−O = 2.429(8) Å) and the remaining 30 at site II (Ca−O = 2.276(5) Å). In Ba_{46}−X, Ba^{2+} ions are again found at three sites: 14.5 per unit cell are at site I (Ba−O = 2.778(11) Å), only 1.5 are at site I′ (Ba−O = 2.44(3) Å), and 30 are at site II (Ba−O = 2.667(8) Å). In the three crystals, sites I and II are the most populated; sites I′ and II′, if they were used, are only sparsely occupied. Ca^{2+} appears to fit the octahedral site I best. No cations are found at sites III or III′, all of which are clearly less favorable for alkaline-earth cations in dehydrated zeolite X.

Introduction

The crystal structure of sodium zeolite X in its hydrated form was determined by Broussard and Shoemaker[1] using powder X-ray diffraction techniques. It was reinvestigated by single-crystal methods.[2] The distribution and coordination of various cations in the frameworks of faujasite-type zeolites have been widely investigated and reviewed.[3]

Only a few studies of dehydrated Group II cation-exchanged zeolite X are present in the literature.[4−9] Anderson *et al.*[4] determined the crystal structure of hydrated and fully dehydrated $Mg_{31}Na_{30}$−X and $Mg_{23}Ca_{23}$−X. Their results are summarized in Table 1. Smolin *et al.*[5] determined the crystal structures of Ca−X after dehydration at various temperatures. In a partially dehydrated form, Ca^{2+} ions are located in sites I, I′, II, and III; see Table 1. They confirmed that the occupancy at site III decreases with increasing dehydration temperature. In partly dehydrated $Sr_{44.8}$−X[6], Sr^{2+} ions are located in four sites: I, I′, II, and II′. Barrer *et al.*[7] reported that Ba^{2+} (r = 1.34 Å) did not exchange completely into zeolite X at room temperature and that it did not occupy site I in the hydrated zeolite. In a dehydrated crystal of Ba^{2+}-exchanged natural faujasite[8] and in dehydrated $Ba_{38}Na_{10}$−X,[9] Ba^{2+} ions occupy sites I, I′, and II. The order of decreasing occupancy of sites for the Ba^{2+} ion is II > I > I′.

Frei *et al.* have studied the visible-light-induced oxidation of small olefins by O_2 in alkali- and alkaline-earth-exchanged zeolite matrices.[10,11] The reactions are very selective and lead to the corresponding alkene hydroperoxide in each case. Laser reaction excitation spectra (measurement of the product growth as a function of CW dye laser wavelength) revealed a continuous absorption tail in the visible spectral region for each system. They attributed this absorption to an alkene·O_2 contact charge-transfer transition. In the visible range, diffuse reflectance spectroscopy has been used to measure alkene−oxygen charge-transfer absorption in Na−Y and Ba−Y and to determine the

TABLE 1: Distribution of Group II Cations over Sites (Previous Work)

		sites					
crystals		I	I′	II	II′	III	total no.
h-Mg,Na−X[a,b]	Mg^{2+}		7.4		4.2	8	19.6
	Na^+	5	9.3	7			21.3
d-Mg,Na−X[b,c]	Mg^{2+}	5	9		15.9		29.9
	Na^+	5	6	15			26
h-Mg,Ca−X[a,b]	Mg^{2+}		2.9		5.8		8.7
	Ca^{2+}		16.5		1.9		18.4
d-Mg,Ca−X[b,c]	Mg^{2+}			14.4	8		22.4
	Ca^{2+}	12.3	3.8		7.0		23.1
h-Ca_{46}−X[a,d]	Ca^{2+}		20.1	10.5		16.5	47.1
d-Ca_{46}−X[c,d]	Ca^{2+}	14.6	2.6	29.0		2.7	48.9
d-$Sr_{44.8}$−X[e,f]	Sr^{2+}	6.1	12.0	20.3	6.4		44.8
d-Ba−faujasite[g,h]	Ba^{2+}	7.3	5.0	11.3			23.6

[a] Hydrated. [b] Reference 4. [c] Dehydrated at 400 °C. [d] Reference 5. [e] Dehydrated at 680 °C. [f] Reference 6. [g] Dehydrated at 500 °C. [h] Reference 8; no entry is made for dehydrated $Ba_{38}Na_{10}$−X (ref 9) because those results are not quantitative.

[⊗] Abstract published in *Advance ACS Abstracts,* July 15, 1997.

S1089-5647(97)00907-3 CCC: $14.00

photooxygenation quantum efficiencies.[12] A principal result of their study is the direct evidence, by diffuse reflectance spectroscopy, for a very strong stabilization of alkene·O_2 charge-transfer states in the ionic environment of a zeolite Y cage. The largest electric field gradients in the zeolite are near the exchangeable cations, so it is expected that their charge, radii, and the sites they select should govern the function of those catalysts.

Sun *et al.*[13] used Ba−Y and Ca−Y for the oxidation of toluene. They reported the first selective photooxidation of toluene to benzaldehyde by O_2. It was accomplished by photoexcitation of $C_6H_5CH_3$·O_2 complexes in the molecular-scale cages of alkaline-earth-exchanged faujasitic zeolites with visible light. Blatter *et al.*[14,15] used Ba−Y for the oxidation of propylene and for the highly selective formation of *tert*-butylhydroperoxide from isobutane. In catalysis, photochemical means are attractive because reaction surfaces can be accessed selectively and the reactions can occur at ambient temperature.

This work was done to learn the site selectivities of the three common alkaline-earth cations in fully dehydrated zeolite X. These selectivities should depend strongly upon ionic radius.

Experimental Section

Large single crystals of sodium zeolite X, stoichiometry $Na_{92}Si_{100}Al_{92}O_{384}$ per unit cell, were prepared in St. Petersburg, Russia.[16] For each of the following preparations, one of these, a colorless octahedron about 0.2 mm for Ca_{46}−X and Ba_{46}−X and 0.25 mm for $Mg_{46}(H_2O)_4$−X in cross section, was lodged in a fine Pyrex capillary.

The crystals of $Mg_{46}(H_2O)_4$−X, Ca_{46}−X, and Ba_{46}−X were obtained by ion exchange with 0.05 M $MgCl_2$·$6H_2O$ (Aldrich, 99.995%), 0.05 M $Ca(NO_3)_2$ (Aldrich, 99.997%), and 0.05 M $Ba(OH)_2$·H_2O (Aldrich, 99%), respectively. For each crystal, ion exchange was accomplished by flow methods; the exchange solution was allowed to flow past each crystal at a velocity of approximately 1.5 cm/s for 5 d at room temperature.

The crystals of Ca^{2+}- and Ba^{2+}-exchanged zeolite X were dehydrated by slowly increasing the temperature by 25 °C per hour to 370 °C, followed by 48 h at 370 °C and 2×10^{-6} Torr. Mg^{2+}-exchanged zeolite X was dehydrated similarly, but at 250 °C. (Two other Mg^{2+}-exchanged zeolite X crystals, similarly dehydrated at 370 and 300 °C, had cracked.)

After cooling to room temperature, each crystal, still under vacuum, was sealed in its Pyrex capillary by torch. The crystals of $Mg_{46}(H_2O)_4$−X and Ca_{46}−X were colorless; Ba_{46}−X was yellow.

X-ray Data Collection

The cubic space group $Fd\bar{3}$ was used throughout this work. This choice is supported by (a) the low Si/Al ratio, which in turn requires, at least in the short range, alternation of Si and Al, and (b) the observation that this crystal, like all other crystals from the same batch, does not have intensity symmetry across (110) and therefore lacks that mirror plane. Molybdenum K_α radiation was used for all experiments ($K\alpha_1$, $\lambda = 0.709\,30$ Å; $K\alpha_2 = 0.71359$ Å). The unit cell constants at 21(1) °C, each determined by least-squares refinement of 25 intense reflections for which $14° < 2\theta < 24°$, are $a = 24.671(5)$ Å for dehydrated $Mg_{46}(H_2O)_4$−X, 25.024(4) Å for dehydrated Ca_{46}−X and 22.266(5) Å for dehydrated Ba_{46}−X. The intensities of all lattice points for which $2\theta < 50°$ were recorded. Of the 1340, 1400, and 1576 unique reflections measured for $Mg_{46}(H_2O)_4$−X, Ca_{46}−X, and Ba_{46}−X, only the 439, 434, and 485 unique reflections, respectively, for which $I > 3\sigma(I)$, were used in subsequent structure determinations.

Absorption corrections (for the $Mg_{46}(H_2O)_4$−X crystal, $\mu R = 0.048$ and $\rho_{cal} = 1.40$ g/cm^{-3}; for the Ca_{46}−X crystal, $\mu R = 0.077$ and $\rho_{cal} = 1.41$ g/cm^3; for the Ba_{46}−X crystal, $\mu R = 0.322$ and $\rho_{cal} = 1.82$ g/cm^3)[17] were made empirically using a ψ scan. The calculated adjusted transmission coefficients ranged from 0.96 to 0.999 for the three crystals. These corrections had little effect on the final R indices. Other details are the same as previously reported.[18]

Structure Determination

(a) Partially Dehydrated $Mg_{46}(H_2O)_4$−X. Full-matrix least-squares refinement was initiated with the atomic positions of the framework atoms [Si, Al, O(1), O(2), O(3), and O(4)] of dehydrated Ca,Mg−X.[4] Anisotropic refinement converged to an R_1 index, $(\sum(|F_o| - |F_c|)/\sum F_o)$, of 0.19 and a weighted R_2 index, $(\sum w(F_o - |F_c|)^2/\sum wF_o^2)^{1/2}$ of 0.24.

A difference Fourier function revealed three large peaks, at (0.0, 0.0, 0.0), (0.20, 0.20, 0.20), and (0.23, 0.23, 0.23), with heights of 10.0, 7.2, and 2.6 e Å^{-3}, respectively. Refinement including them as Mg^{2+} ions with anisotropic temperature factors at Mg(1) and Mg(4), and isotropically at Mg(3), respectively, converged to $R_1 = 0.054$ and $R_2 = 0.057$ (see Table 2a).

On an ensuing difference Fourier function, a peak of height 1.6 e Å^{-3} appeared at (0.057, 0.057, 0.057). Least-squares refinement including this peak isotropically as Mg(2) converged to $R_1 = 0.050$ and $R_2 = 0.051$. From a subsequent difference Fourier function, a peak of height 0.6 e Å^{-3} was found at (0.146, 0.146, 0.146), which was refined as O(5). The occupancy numbers at Mg(1), Mg(2), Mg(3), and Mg(4) were reset and fixed as in the last column of Table 2a because (1) the number of ions at Mg(1) plus half the number at Mg(2) cannot exceed 16 per unit cell (otherwise an impossibly short site I to I′ distance would exist) and (2) the total number must be 46 per unit cell (to balance the −92 charge of the zeolite framework). The occupancy at O(5) was fixed at 4.0, equal to that at Mg(3), because the distance involved indicates that O(5) represents coordinated water molecules. The relatively large displacement (0.64(1) Å) of Mg(3) from the plane of the three O(2) oxygens to which it coordinates supports this result (see Table 5). The final error indices converged to $R_1 = 0.048$ and $R_2 = 0.046$. The final difference Fourier function was featureless.

(b) Dehydrated Ca_{46}−X. Full-matrix least-squares refinement was initiated with the positional and thermal parameters of the framework atoms in partially dehydrated $Mg_{46}(H_2O)_4$−X. Isotropic refinement of the framework atoms converged to $R_1 = 0.29$ and $R_2 = 0.30$.

The initial difference Fourier function revealed large peaks at (0.0, 0.0, 0.0) and (0.22, 0.22, 0.22) with heights of 14.7 and 10.0 e Å^{-3}, respectively. Anisotropic refinement including these peaks as Ca^{2+} ions at Ca(1) and Ca(2), respectively, converged to $R_1 = 0.042$ and $R_2 = 0.037$ (see Table 2b). Occupancy refinement converged at 16.2(1) and 29.4(2), respectively. These values were reset and fixed at 16.0 ions at Ca(1), its maximum value, and 30.0 at Ca(2), to complete a total of 46 Ca^{2+} ions per unit cell. Anisotropic refinement of the framework atoms and Ca^{2+} ions converged to $R_1 = 0.042$ and $R_2 = 0.037$. The final difference Fourier function was featureless.

(c) Dehydrated Ba_{46}−X. Full-matrix least-squares refinement began with the atomic and thermal parameters of the framework atoms in dehydrated Ca_{46}−X. Anisotropic refinement converged to $R_1 = 0.48$ and $R_2 = 0.52$.

A difference Fourier function showed the positions of the Ba^{2+} ions at (0.24, 0.24, 0.24), Ba(3), with peak height 10.8 e Å^{-3}, and those at (0.0, 0.0, 0.0), Ba(1), with peak height 10.4 e Å^{-3}. Anisotropic refinement of the framework atoms and

TABLE 2: Positional, Thermal,[a] and Occupancy Parameters

atom	wyc. pos.	site	x	y	z	U_{11}[b] or U_{iso}	U_{22}	U_{33}	U_{12}	U_{13}	U_{23}	occupancy[c] varied	occupancy[c] fixed
(a) Partially Dehydrated $Mg_{46}(H_2O)_4-X$													
Si	96(g)		−520(1)	1227(1)	339(1)	186(11)	133(10)	179(11)	−1(13)	−7(11)	−27(14)		96
Al	96(g)		−539(1)	377(1)	1211(1)	189(12)	163(12)	133(12)	17(11)	3(14)	−22(14)		96
O(1)	96(g)		−1115(2)	20(3)	1063(2)	262(40)	558(42)	321(39)	−156(35)	−1(28)	−85(36)		96
O(2)	96(g)		−29(3)	−27(3)	1471(2)	231(31)	287(32)	199(30)	104(28)	7(29)	−35(30)		96
O(3)	96(g)		−313(2)	635(3)	583(3)	274(33)	209(33)	360(35)	67(32)	70(34)	140(30)		96
O(4)	96(g)		−655(2)	843(2)	1694(2)	365(36)	243(33)	215(33)	−21(35)	3(35)	−85(29)		96
Mg(1)	16(c)	I	0	0	0	312(20)	312(20)	312(20)	42(24)	42(24)	42(24)	13.8(2)	14
Mg(2)	32(e)	I′	585(9)	585(9)	589(9)	287(98)	287(98)	287(98)	27(122)	27(122)	27(122)	4.0(3)	4
Mg(3)	32(e)	II′	2026(8)	2026(8)	2026(8)	132(80)[d]						3.8(3)	4
Mg(4)	32(e)	II	2288(2)	2288(2)	2288(2)	532(22)	532(22)	532(22)	227(26)	227(26)	227(26)	26.2(4)	24
O(5)	32(e)	II′	1450(24)	1450(24)	1450(24)	1141(761)[d]							4
(b) Dehydrated $Ca_{46}-X$													
Si	96(g)		−540(1)	1230(1)	335(1)	115(11)	105(11)	90(11)	−16(14)	−8(12)	−15(16)		96
Al	96(g)		−567(1)	366(1)	1215(1)	94(12)	105(12)	94(12)	32(12)	−14(14)	−35(16)		96
O(1)	96(g)		−1130(2)	5(3)	1069(2)	145(35)	202(31)	166(34)	−69(34)	−27(25)	−59(32)		96
O(2)	96(g)		−37(3)	−31(3)	1429(2)	125(28)	117(30)	161(30)	27(30)	−30(30)	−43(31)		96
O(3)	96(g)		−361(2)	662(2)	611(2)	174(32)	66(31)	150(31)	30(31)	14(32)	−20(28)		96
O(4)	96(g)		−595(2)	798(2)	1734(2)	330(35)	124(31)	148(33)	−119(35)	67(37)	−116(28)		96
Ca(1)	16(c)	I	0	0	0	123(10)	123(10)	123(10)	1(13)	1(13)	1(13)	16.2(1)	16
Ca(2)	32(e)	II	2234(1)	2234(1)	2234(1)	288(10)	288(10)	288(10)	91(13)	91(13)	91(13)	29.4(2)	30
(c) Dehydrated $Ba_{46}-X$													
Si	96(g)		−559(2)	1253(2)	340(2)	68(18)	60(17)	54(18)	27(26)	6(17)	−13(25)		96
Al	96(g)		−575(2)	363(2)	1246(2)	56(19)	3(19)[e]	54(18)	22(18)	−14(27)	−3(27)		96
O(1)	96(g)		−1118(4)	3(5)	1081(4)	180(64)	63(50)	146(59)	−23(51)	25(42)	26(48)		96
O(2)	96(g)		−43(4)	−46(4)	1371(3)	82(51)	125(52)	140(65)	31(46)	0(49)	−110(51)		96
O(3)	96(g)		−394(4)	743(4)	708(4)	56(54)	157(60)	136(59)	9(52)	69(51)	−17(52)		96
O(4)	96(g)		−629(4)	700(4)	1826(4)	41(49)	96(55)	116(56)	−28(51)	36(51)	−64(47)		96
Ba(1)	16(c)	I	0	0	0	268(7)	268(7)	268(7)	69(8)	69(8)	69(8)	14.5(1)	14.5
Ba(2)	32(e)	I′	530(10)	530(10)	530(10)	213(4)	213(4)	213(4)	97(6)	97(6)	97(6)	1.5(1)	1.5
Ba(3)	32(e)	II	2409(1)	2409(1)	2409(1)	213(4)	213(4)	213(4)	97(6)	97(6)	97(6)	29.6(1)	30

[a] Positional and anisotropic thermal parameters are given $\times 10^4$. Numbers in parentheses are the esd's in the units of the least significant digit given for the corresponding parameter. [b] The anisotropic temperature factor $= \exp[-2\pi^2(h^2(a^*)^2U_{11} + k^2(b^*)^2U_{22} + l^2(c^*)^2U_{33} + 2hk(a^*b^*)U_{12} + 2hl(a^*c^*)U_{13} + 2kl(b^*c^*)U_{23})]$. [c] Occupancy factors are given as the number of atoms or ions per unit cell. [d] $U_{iso} = (B_{iso}/8\pi^2)$. [e] This physically unacceptable value was increased by 1σ in the preparation of Figures 7−9.

isotropic refinement of the Ba^{2+} ions converged to $R_1 = 0.042$ and $R_2 = 0.047$.

From a subsequent difference Fourier function, a peak of height 1.0 e Å^{-3} was found at (0.052, 0.052, 0.052), which was refined as Ba(2). The thermal motion of Ba(2) was unreasonably large, so the anisotropic thermal parameters of Ba(2) were constrained to be equal to those of Ba(3); the occupancy at Ba(2) was also constrained so that the total occupancy at Ba(1) and Ba(2) would equal 16. Anisotropic refinement of the framework atoms and Ba^{2+} ions at Ba(1), Ba(2) and Ba(3) converged to $R_1 = 0.046$ and $R_2 = 0.048$. The occupancy numbers of Ba(1), Ba(2) and Ba(3) were reset and fixed as in the last column of Table 2c. The final error indices converged to $R_1 = 0.046$ and $R_2 = 0.049$. The final difference Fourier function was featureless except for a peak of height 1.1(1) e Å^{-3} at (0.33, 0.33, 0.33); this peak was far from other atoms and was unstable in least squares.

The goodness-of-fit, $(\sum w(F_o - |F_c|)^2/(m - s))^{1/2}$, is 2.09, 1.48, and 1.87 for $Mg_{46}(H_2O)_4-X$, $Ca_{46}-X$, and $Ba_{46}-X$, respectively; m (439, 434, and 485, respectively) is the number of observations, and s (66, 60, and 62, respectively) is the number of variables in least squares. All shifts in the final cycles of least-squares refinement were less than 0.1% of their corresponding standard deviations.

Atomic scattering factors for Si, Al, O^-, Mg^{2+}, Ca^{2+}, and Ba^{2+} were used. Atomic scattering factors were modified to account for anomalous dispersion. The final structural parameters and selected interatomic distances and angles are presented in Tables 2 and 3.

Discussion

Zeolite X is a synthetic counterpart of the naturally occurring mineral faujasite. The 14-hedron with 24 vertices known as the sodalite cavity or β-cage may be viewed as the principal building block of the aluminosilicate framework of the zeolite (see Figure 1). These β-cages are connected tetrahedrally at six-rings by bridging oxygens to give double six-rings (D6Rs, hexagonal prisms) and, concomitantly, to give an interconnected set of even larger cavities (supercages) accessible in three dimensions through 12-ring (24-membered) windows. The Si and Al atoms occupy the vertices of these polyhedra. The oxygen atoms lie approximately halfway between each pair of Si and Al atoms but are displaced from those points to give near tetrahedral angles about Si and Al.

Exchangeable cations, which balance the negative charge of the aluminosilicate framework, are found within the zeolite's cavities. They are usually found at the following sites shown in Figure 1: site I at the center of a D6R (alternatively called the hexagonal prism), site I′ in the sodalite (β) cavity on the opposite side of one of the D6Rs 6-rings from site I, II′ inside the sodalite cavity near a single 6-ring (S6R) entrance to the supercage, II in the supercage adjacent to a S6R, III in the supercage opposite a 4-ring between two 12-rings, and III′ somewhat off III (off the 2-fold axis).[19,20]

The structures of $Mg_{46}(H_2O)_4-X$, $Ca_{46}-X$, and $Ba_{46}-X$ appear to be fully exchanged and either fully anhydrous or stoichiometrically partially dehydrated. Because of this, these structures are relatively simple.

(a) Partially Dehydrated $Mg_{46}(H_2O)_4-X$. In $Mg_{46}(H_2O)_4-X$, the Mg^{2+} ions are found at four crystallographic sites. About

TABLE 3: Selected Interatomic Distances (Å) and Angles (deg)[a]

	Framework		
	$Mg_{46}(H_2O)_4-X$	$Ca_{46}-X$	$Ba_{46}-X$
Si−O(1)	1.629(6)	1.594(6)	1.615(11)
Si−O(2)	1.631(6)	1.654(7)	1.646(11)
Si−O(3)	1.659(6)	1.641(6)	1.643(11)
Si−O(4)	1.603(6)	1.623(7)	1.628(12)
average	1.630(6)	1.628(6)	1.633(11)
Al−O(1)	1.712(6)	1.715(6)	1.698(11)
Al−O(2)	1.729(6)	1.743(7)	1.723(11)
Al−O(3)	1.764(7)	1.759(6)	1.726(12)
Al−O(4)	1.681(6)	1.693(7)	1.701(12)
average	1.722(6)	1.728(6)	1.709(12)
O(1)−Si−O(2)	111.9(3)	112.7(4)	111.4(6)
O(1)−Si−O(3)	107.5(3)	108.4(3)	110.3(6)
O(1)−Si−O(4)	109.3(3)	113.7(3)	111.6(6)
O(2)−Si−O(3)	107.4(3)	106.7(3)	105.9(5)
O(2)−Si−O(4)	108.1(3)	102.8(3)	103.7(5)
O(3)−Si−O(4)	112.7(3)	112.2(3)	113.6(6)
O(1)−Al−O(2)	112.8(3)	113.0(3)	110.7(5)
O(1)−Al−O(3)	105.0(3)	106.3(3)	108.6(6)
O(1)−Al−O(4)	111.2(3)	117.8(3)	114.5(5)
O(2)−Al−O(3)	107.7(3)	106.4(3)	105.7(5)
O(2)−Al−O(4)	104.8(3)	99.2(3)	101.9(5)
O(3)−Al−O(4)	115.5(3)	113.7(3)	114.8(5)
Si−O(1)−Al	126.5(4)	125.9(4)	131.1(7)
Si−O(2)−Al	134.2(4)	140.8(4)	153.9(6)
Si−O(3)−Al	122.6(4)	130.2(3)	144.5(7)
Si−O(4)−Al	158.1(4)	169.2(4)	149.4(7)

	Cations and Framework				
$Mg_{46}(H_2O)_4-X$		$Ca_{46}-X$		$Ba_{46}-X$	
Mg(1)−O(3)	2.262(6)	Ca(1)−O(3)	2.429(8)	Ba(1)−O(3)	2.778(11)
Mg(2)−O(3)	2.221(5)			Ba(2)−O(3)	2.44(3)
Mg(3)−O(2)	2.223(12)	Ca(2)−O(2)	2.276(5)	Ba(3)−O(2)	2.667(8)
Mg(3)−O(5)	2.48(4)				
Mg(4)−O(2)	2.184(5)				
O(3)−Mg(1)−O(3)	90.8(2)/89.2(2)	O(3)−Ca(1)−O(3)	93.4(2)/86.6(2)	O(3)−Ba(1)−O(3)	92.1(3)/87.9(3)
O(3)−Mg(2)−O(3)	93.0(6)			O(3)−Ba(2)−O(3)	110.1(8)
O(2)−Mg(3)−O(2)	112.1(8)	O(2)−Ca(2)−O(2)	118.3(2)	O(2)−Ba(3)−O(2)	103.7(3)
O(2)−Mg(4)−O(2)	115.2(3)				

[a] Numbers in parentheses are estimated standard deviations in the units of the least significant digit given for the corresponding value.

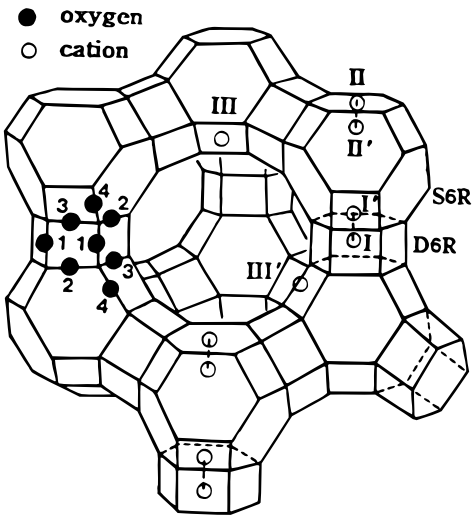

Figure 1. Stylized drawing of the framework structure of zeolite X. Near the center of each line segment is an oxygen atom. The different oxygen atoms are indicated by the numbers 1−4. Silicon and aluminum atoms alternate at the tetrahedral intersections, except that Si substitutes for about four of the Al's per unit cell. Extraframework cation positions are labeled with Roman numerals.

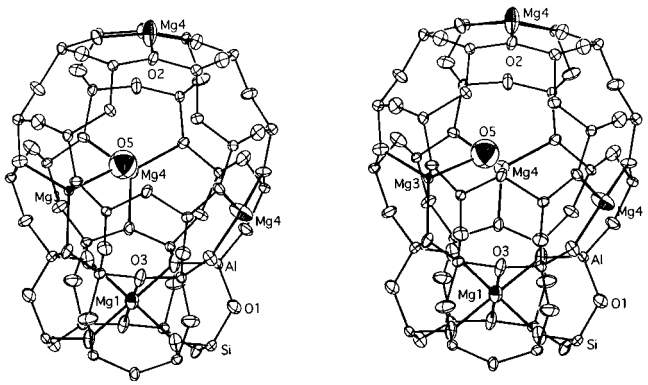

Figure 2. Stereoview of a sodalite cavity with an attached D6R in dehydrated $Mg_{46}(H_2O)_4-X$. One Mg^{2+} ion at Mg(1) (site I), one Mg^{2+} ion at Mg(3) (site II′), and three Mg^{2+} ions at Mg(4) (site II) are shown. Ellipsoids of 20% probability are used.

14 Mg^{2+} ions at Mg(1) occupy the 16-fold site I (see Figure 2). The octahedral Mg(1)−O(3) distance, 2.262(6) Å, is much longer than the sum of the ionic radii of Mg^{2+} and O^{2-}, 0.66 + 1.32 = 1.98 Å,[21a] and is longer than 2.12 Å, the Mg−O distance in MgO (NaCl structure).[21b] For comparison, the $Mg^{2+}-O(3)$ distance is 2.28(1) Å in dehydrated $Mg_{31}Na_{30}-X$[4]. A similar distance, 2.26(1) Å, was observed in $Mg_{1.5}Na_9-A$.[22] (In both $Mg_{31}Na_{30}-X$ and $Mg_{1.5}Na_9-A$, only some sort of average O(3) position was refined, so the corresponding $Mn^{2+}-O$ distances should be somewhat elongated and inaccurate in those structures.)-

Four Mg^{2+} ions at Mg(2) are found at site I′; each is recessed *ca*. 1.21(1) Å into the sodalite unit from its three−O(3) plane (see Table 5). Each Mg^{2+} ion coordinates at 2.221(5) Å to those three oxygens. The shortest approach distance between the I

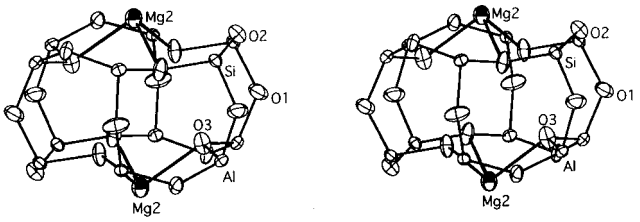

Figure 3. Stereoview of the less common D6R in dehydrated $Mg_{46}(H_2O)_4-X$. Two Mg^{2+} ions at Mg(2) (site I′) are shown. Ellipsoids of 20% probability are used.

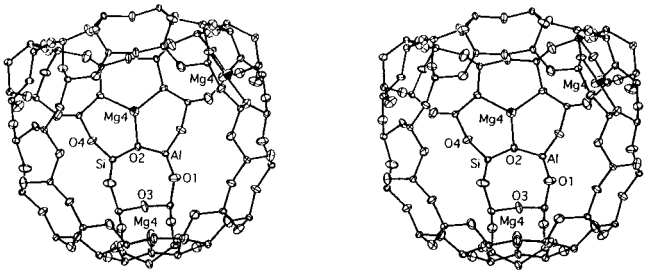

Figure 4. Stereoview of a supercage in dehydrated $Mg_{46}(H_2O)_4-X$. Three Mg^{2+} ions at Mg(4) (site II) are shown. About 50% of the supercages have this arrangement. The remaining 50% of the supercages have one Mg^{2+} ion at Mg(3) and three Mg^{2+} ions at Mg(4). Ellipsoids of 20% probability are shown.

and I′ sites is only 2.50 Å, which must be avoided because of electrostatic repulsion. Therefore if a site I is occupied, the two adjacent site I′s (of the same D6R) cannot be. It follows that the four Mg(2) ions must lie outside those two D6Rs per unit cell that are void of Mg(1) ions (see Figure 3). The 5.0 Å repulsive interaction between the two Mg(2) ions of a single D6R is responsible for the longer Mg−O distance (as compared to that for Mg(4)) and greater displacement from the three−O(3) plane than even Ba^{2+} with its much larger cationic radius (Ba(2) in $Ba_{46}-X$, *vide infra*).

Four Mg^{2+} ions lie at Mg(3) (site II′) and the remaining 24 Mg^{2+} ions lie at Mg(4) (site II). Mg(3) is recessed *ca.* 0.64(1) Å into sodalite cavity and Mg(4) is recessed 0.48(1) Å into the supercage from the S6R plane at O(2) (see Figures 2 and 4 and Table 5). Each of these Mg^{2+} ions coordinates to three O(2) oxygens at 2.223(12) and 2.184(5) Å, respectively, again longer than the sum of the ionic radii, 1.98 Å. It is very unusual for an ion with so low a coordination number to be so distant from its nearest neighbors. (This is true for the ions at Mg(2) also.) Each Mg(3) coordinates further to a water molecule at O(5) ($Mg^{2+}-OH_2$ = 2.47(3) Å).

Each sodalite cavity contains a Mg^{2+} ion. In half of the sodalite cavities, it is at site I′ (Mg(2)), and in the other half, it and a coordinated water molecule (Mg(3)−O(5)) are at site II′.

The Mg^{2+} ions preferentially occupy sites I and II. Yet neither site is filled. This may be a consequence of the four Si atoms per unit cell that must be at Al, a 96-fold position which contains 92 Al and 4 Si atoms. The small size of the Mg^{2+} ion allows it to fit comfortably within the D6R (site I), so this site is not unsuitable because it is too small; it may be too large.

The O(3)−Mg(1)−O(3) bond angles are 90.8(2)° and 89.2(2)°, nearly octahedral. The O(3)−Mg(2)−O(3) bond angles are 93.0(6)°, far from trigonal planar due to the repulsion between Mg^{2+} ions at sites I′. Mg(3) and Mg(4) are much closer to trigonal planar (see Table 3). The cation distribution is summarized in Table 4.

$Mg_{46}(H_2O)_4-X$ is sensitive to dehydration temperature. The crystal studied survived dehydration at 250 °C, but two crystals dehydrated at higher temperatures had cracked. The relatively low structural stability of Mg^{2+}-exchanged zeolite X at high temperature may be related to the large distortions of the framework (strain) occurring upon dehydration. The magnitude of the distortion can be seen in the framework angles at O(2) and O(3), which are less than the corresponding angles for $Ca_{46}-X$ and $Ba_{46}-X$ (see Table 3). It can also be seen in the cell constant of dehydrated $Mg_{46}(H_2O)_4-X$: at 24.671(5) Å, it is sharply less than those of $Ca_{46}-X$ and $Ba_{46}-X$.

TABLE 4: Distribution of Cations over Sites

	crystals		
sites	$Mg_{46}(H_2O)_4-X$	$Ca_{46}-X$	$Ba_{46}-X$
I	14	16	14.5
I′	4	0	1.5
II	24	30	30
II′	4		

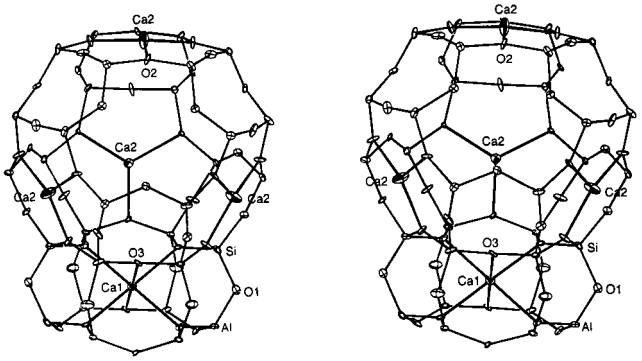

Figure 5. Stereoview of a sodalite cavity with an attached D6R in dehydrated $Ca_{46}-X$. One Ca^{2+} ion at Ca(1) (site I) and four Ca^{2+} ions at Ca(2) (site II) are shown. Ellipsoids of 20% probability are used.

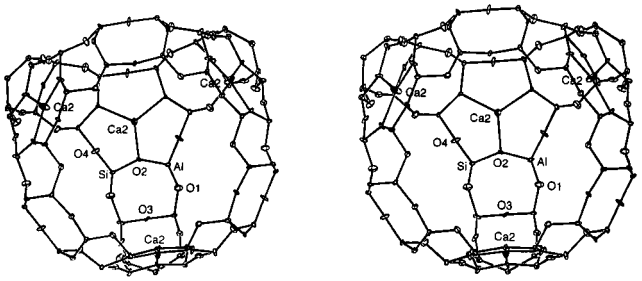

Figure 6. Stereoview of a supercage in dehydrated $Ca_{46}-X$. Four Ca^{2+} ions at Ca(2) (site II) are shown. About 75% of the supercages have this arrangement. The remainder have only three Ca^{2+} ions. Ellipsoids of 20% probability are shown.

(b) Dehydrated $Ca_{46}-X$. This structure was determined twice using separately prepared crystals. In the first determination, 166 reflections were refined to R_1 = 0.096 and R_2 = 0.068; a = 25.002(1) Å. The work was repeated more carefully to increase the precision of the results, and only the latter work is presented fully in this report. The only difference between the two structures is a small one in the cell constant.

In $Ca_{46}-X$, all Ca^{2+} ions are located with high occupancy at just two crystallographic sites. The 16 Ca^{2+} ions at Ca(1) fill site I at the center of the D6Rs (see Figure 5). The octahedral Ca(1)−O(3) distance, 2.429(8) Å, is just a little longer than the sum of the corresponding ionic radii, 0.99 + 1.32 = 2.31 Å,[21a] indicating a reasonably good fit. The 30 Ca^{2+} ions at Ca(2) are located at site II in the supercage; each coordinates trigonally at 2.276(5) Å to three O(2) framework oxygens and is recessed *ca.* 0.30(1) Å into the supercage from their plane (see Figures 5 and 6 and Table 5). The O(2)−Ca(2)−O(2) bond angle (118.3(2)°, near trigonal planar) indicates that Ca^{2+} fits this six-ring well. Clearly site I, because it is filled, is preferred over site II.

Smolin *et al.*[5] investigated the migration of cations in fully Ca^{2+}-exchanged zeolite X during dehydration by heating in a

TABLE 5: Displacements of Cations (Å) from Six-Ring Planes

	position	site	displacement
$Mg_{46}(H_2O)_4-X$			
at O(2)[a]			
	Mg(3)	II′[c]	−0.64(1)
	Mg(4)	II	0.48(1)
at O(3)[b]			
	Mg(2)	I′[c]	−1.21(1)
	Mg(1)	I	1.29(1)
$Ca_{46}-X$			
at O(2)[a]			
	Ca(2)	II	0.30(1)
at O(3)[b]	Ca(1)	I	1.32(1)
$Ba_{46}-X$			
at O(2)[a]			
	Ba(3)	II	1.12(1)
at O(3)[b]			
	Ba(2)	I′[c]	−0.79(1)
	Ba(1)	I	1.54(1)

[a] A positive displacement indicates that the ion lies at site II in the supercage. [b] A positive displacement indicates that the ion lies at site I in a double six-ring. [c] Sites I′ and II′ are in the sodalite cavity; their displacements are negative.

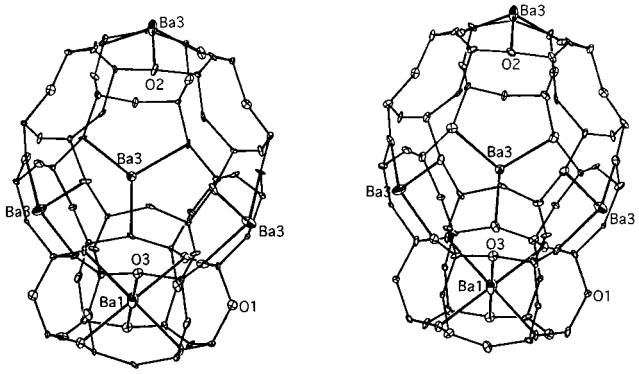

Figure 7. Stereoview of a sodalite cavity with an attached D6R in dehydrated $Ba_{46}-X$. One Ba^{2+} ion at Ba(1) (site I) and four Ba^{2+} ions at Ba(3) (site II) are shown. Ellipsoids of 20% probability are used.

stream of hot N_2 gas. The Ca^{2+} ions progressed into the D6Rs and to S6R sites in the supercage. Their positions after dehydration at 400 °C are indicated in Table 1. The occupancy at site III decreased gradually with increasing dehydration temperature but never reached zero, indicating that full dehydration was never achieved.

The cation distribution found for $Ca_{46}-X$ in this work is much simpler than that reported by Smolin.[5] This same simple distribution was found in dehydrated $Cd_{46}-X$[23] and $Mn_{46}-X$[24] whose crystal structures were recently determined by single-crystal X-ray diffraction methods. This indicates that complete dehydration is being achieved.

(c) Dehydrated $Ba_{46}-X$. In $Ba_{46}-X$, the Ba^{2+} ions are found at three sites, unlike $Ca_{46}-X$. The 14.5 Ba^{2+} ions at Ba(1) lie at site I at D6R centers (see Figure 7). The octahedral Ba(1)−O(3) distance, 2.778(1) Å, is a little longer than the sum of the ionic radii of Ba^{2+} and O^{2-}, 1.34 + 1.32 = 2.66 Å,[21a] as was seen above with the corresponding octahedral Ca^{2+} ions at site I. This 16-fold position is occupied by only 14.5 Ba^{2+} ions, perhaps because this site is a little too small for a large cation like Ba^{2+} (r = 1.34 Å): other smaller divalent cations such as Ca^{2+} (r = 0.99 Å), Mn^{2+} [24] (r = 0.80 Å), Co^{2+} [25] (r = 0.74 Å), and Cd^{2+} [23] (r = 0.97 Å) fully occupy this 16-fold position.

The Ba(2) position is on a 3-fold axis in the sodalite unit, opposite D6Rs at site I′ (see Figure 8). This 32-fold position is occupied by only 1.5 Ba^{2+} ions. Each coordinates at 2.44(3) Å to three O(3) framework oxygens and is recessed *ca*. 0.79 Å into the sodalite cavity from their plane (see Table 5). As with $Mg_{46}(H_2O)-X$, because the closest I to I′ approach is 2.32 Å, if a D6R has a Ba^{2+} ion in it, then the two adjacent I′ sites must be unoccupied. Each of the Ba(2) ions must occupy a I′ site that lies outside an empty D6R. Because only 1.5 empty D6Rs are available per unit cell, a 2 × 2.32 Å = 4.64 Å I′ to I′ distance is being avoided also (see Figure 8). Supporting this conclusion is the observation that the corresponding smaller Mg^{2+} ions are further (1.21 Å) from their six-rings than are these Ba^{2+} ions (0.79 Å) (see Table 5).

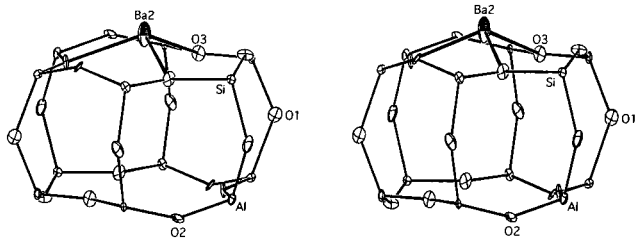

Figure 8. Stereoview of the less common D6R in dehydrated $Ba_{46}-X$. One Ba^{2+} ion at Ba(2) (site I′) is shown. Ellipsoids of 20% probability are used.

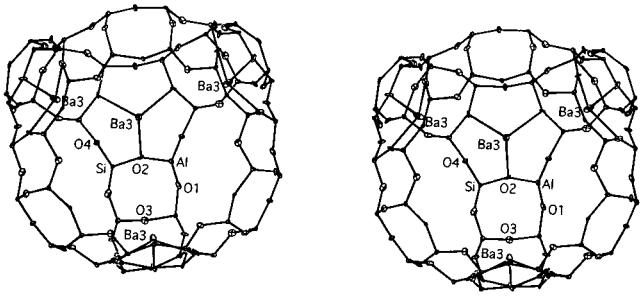

Figure 9. Stereoview of a supercage in dehydrated $Ba_{46}-X$. Four Ba^{2+} ions at Ba(3) (site II) are shown. About 75% of the supercages have this arrangement. The remainder have only three Ba^{2+} ions. Ellipsoids of 20% probability are shown.

The remaining 30 Ba^{2+} ions at Ba(3) lie at site II and are recessed 1.12(1) Å into the supercage from the plane at O(2) (see Figures 7 and 9 and Table 5). Each of these Ba^{2+} ions coordinates to three O(2) oxygens at 2.667(8) Å, the same as the sum of the ionic radii of Ba^{2+} and O^{2-}, 1.34 + 1.32 = 2.66 Å.[21a] The angle subtended at Ba(3), O(2)−Ba(3)−O(2), is 103.7(3)°, far less than trigonal planar, indicating that Ba^{2+} is too large to fit into the plane of this six-ring.

Ba^{2+} has the largest ionic radius (r = 1.34 Å) of any dipositive cation except Ra^{2+} (r = 1.43 Å). However, it is small enough, compared to, for example, Rb^+ and Tl^+ (r = 1.47 Å) and Cs^+ (r = 1.67 Å), for Ba^{2+} ions to fit into the hexagonal prisms, unlike Rb^+, Tl^+,[26] and Cs^+ [27] which cannot.

In dehydrated crystals of Ba^{2+}-exchanged natural faujasite[8] and dehydrated $Ba_{38}Na_{10}-X$[9], all Ba^{2+} ions are located at the same three sites found in this work (see Table 1).

Fully Ba^{2+}-exchanged zeolite X is stable with respect to complete dehydration at high temperature (*ca*. 370 °C). In contrast, the corresponding zeolite A material, although similar in composition, decomposes easily at relatively low temperatures when dehydration is attempted.[28]

MgO and CaO are colorless, but BaO is very pale yellow.[29] This corresponds to the colors of the three crystals whose structures reported here.

(d) Comparisons. The mean values of the Si−O bond lengths for $Mg_{46}(H_2O)_4-X$, $Ca_{46}-X$, and $Ba_{46}-X$ are 1.630(6), 1.628(6), and 1.633(11) Å, respectively. The mean values of the corresponding Al−O bond lengths are appropriately longer: 1.722(6), 1.728(6), and 1.709(12) Å, respectively. The range of individual bond lengths for these three crystals is

wide: Si−O from 1.594(6) to 1.659(6) Å and Al−O from 1.681-(6) to 1.764(7) Å: see Table 3. The individual Si−O and Al−O distances depend upon alkaline-earth cation coordination to framework oxygen: O(1) and O(4) are not involved in coordination; all cations coordinate to O(2) and O(3). Accordingly, the Al−O(1) and Al−O(4) distances are shorter than Al−O(2) and Al−O(3); similarly Si−O(1) and Si−O(4) are shorter than Si−O(2) and Si−O(3) (see Table 3).

The "right" size of the Ca^{2+} ion allows it to occupy site I at the center of the D6R fully; it clearly prefers this position. In partially dehydrated $Mg_{46}(H_2O)_4$−X, Mg^{2+} ions preferentially occupy sites I and II but partially occupy sites I′ and II′. In dehydrated Ca_{46}−X, Ca^{2+} ions occupy only sites I and II. In dehydrated Ba_{46}−X, the Ba^{2+} ions are again located at three sites: I, I′, and II. Ba^{2+} appears to prefer the D6R sites (I and I′) over the S6R site (II).

Mg^{2+} is a little too small, Ca^{2+} fits well, and Ba^{2+} ions are a little too large for site I. Nonetheless, all fit reasonably well into D6Rs. The distribution of cations among sites for the three crystals is presented in Table 4.

The cations at site II are closer to their coordinating oxygens than are those at site I. This is a consequence of their very different coordination numbers, three at site II *vs* six at site I.

In the present work, no cations were found at sites III and III′, which are clearly unfavorable for alkaline-earth cations in dehydrated zeolite X.

Acknowledgment. This work was supported in part by the Basic Research Institute Program, Ministry of Education, Korea, 1995, Project No. BSRI-95-3409.

Supporting Information Available: Tables of observed and calculated structure factors with esd's (45 pages). Ordering information is given on any current masthead page.

References and Notes

(1) Broussard, L.; Shoemaker, D. P. *J. Am. Chem. Soc.* **1960**, *82*, 1041.
(2) Olson, D. H. *J. Phys. Chem.* **1970**, *74*, 14.
(3) Mortier, W. J. *Compilation of Extra-framework Sites in Zeolites*; Butterworth Scientific Ltd.: Guildford, U.K., 1982.
(4) Anderson, A. A.; Shepelev, Yu. F.; Smolin, Yu. I. *Zeolites* **1990**, *10*, 32.
(5) Smolin, Yu. I.; Shepelev, Yu. F.; Anderson, A. A. *Acta Crystallogr., Sect. B* **1989**, *45*, 124.
(6) Olson, D. H., Dempsey, E. *J. Catal.* **1969**, *13*, 221.
(7) Barrer, R. M.; Rees, L. V. C.; Shamsuzzoha, M. *J. Inorg. Nucl. Chem.* **1966**, *28*, 629.
(8) Smith, J. V. Faujasite-Type Structures: Aluminosilicate Framework: Positions of Cations and Molecules: Nomenclature. In *Molecular Sieve Zeolites-I*; Flanigen, E. M., Sand, L. B., Eds.; American Chemical Society: Washington, DC, 1971; p 185.
(9) Godber, J.; Baker, M. O.; Ozin, G. A. *J. Phys. Chem.* **1989**, *93*, 1409.
(10) Blatter, F.; Frei, H. *J. Am. Chem. Soc.* **1993**, *115*, 7501.
(11) Blatter, F.; Frei, H. *J. Am. Chem. Soc.* **1994**, *116*, 1812.
(12) Blatter, F.; Moreau, F.; Frei, H. *J. Phys. Chem.* **1994**, *98*, 13403.
(13) Sun, H.; Blatter, F.; Frei, H. *J. Am. Chem. Soc.* **1994**, *116*, 7951.
(14) Blatter, F.; Sun, H.; Frei, H. *Catal. Lett.* **1995**, *35*, 1.
(15) Blatter, F.; Sun, H.; Frei, H. *Chem. Eur. J.* **1996**, *2*, 113.
(16) Bogomolov, V. N.; Petranovskii, V. P. *Zeolites* **1986**, *6*, 418.
(17) *International Tables for X-ray Crystallography*; Kynoch Press: Birmingham, England, 1974; Vol. II, p 302.
(18) Jang, S. B.; Kim, Y.; Seff, K. *J. Phys. Chem.* **1994**, *98*, 3796.
(19) Sun, T.; Seff, K.; Heo, N. H.; Petranovskii, V. P. *Science* **1993**, *259*, 495.
(20) Sun, T.; Seff, K. *Chem. Rev.* **1994**, *94*, 859.
(21) (a) *Handbook of Chemistry and Physics*, 70th Ed.; The Chemical Rubber Co.: Cleveland, OH, 1989/1990; p F-187. (b) *Handbook of Chemistry and Physics*, 75th Ed.; The Chemical Rubber Co.: Cleveland, OH, 1995; p 12-8.
(22) Kim, Y.; Lee, S. K.; Kim, U. K. *Bull. Korean Chem. Soc.* **1989**, *10*, 349.
(23) Kwon, J. H.; Jang, S. B.; Kim, Y.; Seff, K. *J. Phys. Chem.* **1996**, *100*, 13720.
(24) Jang, S. B.; Jeong, M. S.; Kim, Y.; Seff, K. *J. Phys. Chem.*, submitted for publication.
(25) Yeom, Y. H.; Kim, Y. Unpublished work.
(26) Kim, Y.; Han, Y. W.; Seff, K. *Zeolites*, in press.
(27) Shepelev, Yu. F.; Butikova, I. K.; Smolin, Yu. I. *Zeolites* **1991**, *11*, 287.
(28) Kim, Y.; Subramanian, V.; Firor, R. L.; Seff, K. *ACS Symp. Ser.* **1980**, *135*, 137.
(29) Reference 21b, p 4-43.